



Probabilistic safety assessment of off-site power system under typhoon considering failure correlation between transmission towers

Gungyu Kim ^a, Shinyoung Kwag ^{b,*}, Seunghyun Eem ^{a,*}, Dae-gi Hahm ^c, Jin Hee Park ^d

^a Department of Convergence & Fusion System Engineering, Kyungpook National University, 80, Daehak-ro, Buk-gu, Daegu, 41566, Republic of Korea

^b Department of Civil & Environmental Engineering, Hanbat National University, 125, Dongseo-daero, Yuseong-gu, Daejeon, 34158, Republic of Korea

^c Structural and Seismic Safety Research Team, Korea Atomic Energy Research Institute, 111 Daedeok-daero 989 beon-gil, Yusung-gu, Daejeon, 34057, Republic of Korea

^d Risk and Environmental Safety Research Division, Korea Atomic Energy Research Institute, 111 Daedeok-daero 989 beon-gil, Yusung-gu, Daejeon, 34057, Republic of Korea



ARTICLE INFO

Keywords:

Probabilistic Safety Assessment (PSA)
Off-site Power System
Nuclear Power Plant (NPP)
Typhoon Hazard
Transmission Lines Failure
Failure Correlation
High Wind Failure Probability

ABSTRACT

High-intensity typhoons can cause failure to the structures, systems, and components of nuclear power plants (NPPs) and off-site power systems. Instances have occurred where failure of the off-site power system caused by typhoons has affected NPPs. The off-site power system has been in cases where a typhoon failed multiple transmission towers. In Korea, transmission towers have similar design criteria and material properties and experience similar wind characteristics, leading to a correlation in their failure probabilities. Assuming independent or totally dependent failure probabilities among the transmission towers is unrealistic. For a realistic PSA of the off-site power system due to typhoon-induced high winds, it is necessary to consider an appropriate failure correlation. This study performed a PSA of an off-site power system due to typhoon-induced high winds, considering the failure correlation between transmission towers. The failure correlation between transmission towers based on distance was calculated. The wind fragility of the off-site power system was convolved with the typhoon-induced high-wind hazard at the Kori NPP to calculate the probability of the NPP losing its power supply. Thus, applying the failure correlation of typhoon-induced high winds to the PSA of the off-site power system is considered realistic.

1. Introduction

According to reports by the Intergovernmental Panel on Climate Change (IPCC) and the United Nations Office for International Strategy for Disaster Reduction (UNISDR), the intensity and frequency of typhoons are increasing due to climate change [1–3]. The “Korean Climate Change Assessment Report 2020” indicates a gradual increase in temperature, precipitation, the frequency of typhoons, sea water temperature, and sea level in Korea. Consequently, the frequency and intensity of typhoons in Korea are expected to increase [4]. Typhoons failure the structures, systems, and components (SSCs) of nuclear power plants (NPPs), leading to loss of off-site power (LOOP) events [5,6]. Off-site power systems contribute to the normal and safe operation of NPPs by supplying or receiving power [7]. Currently, NPPs do not account for the failure to off-site power systems caused by typhoon-induced high winds.

However, owing to climate change, such failure may occur more frequently, which can affect the safe operation of NPPs.

In 1992, Hurricane Andrew severely failed the off-site power system of the Turkey Point NPP [8,9]. In South Korea, the Kori NPP was shut down because of the failure of the off-site power system, specifically multiple transmission towers, caused by Typhoon Maemi [10]. Aside from the LOOP events at NPPs, there have been other cases of power system failure caused by typhoon-induced high winds [11,12]. In 2015, Typhoon Mujigae in China failed many transmission towers [13]. In 2014, Typhoon Rammasun in China failed the 110 kV power system, causing a cascading failure between two transmission towers in three sections, which resulted in the collapse of 13 transmission towers [14]. Multiple typhoons have similarly failed numerous transmission towers in the power systems [15]. Therefore, it is unrealistic to consider the transmission towers as independent or totally dependent when

* Corresponding author.

** Co-corresponding author.

E-mail addresses: gungyu819@knu.ac.kr (G. Kim), skwag@hanbat.ac.kr (S. Kwag), eemsh@knu.ac.kr (S. Eem), dhahm@kaeri.re.kr (D.-g. Hahm), jhpark6@kaeri.re.kr (J.H. Park).

performing a probabilistic safety assessment (PSA) [16]. For a realistic PSA of a power system, it is necessary to apply an appropriate correlation [17].

PSA is one of the methods used to assess and manage the safety of a specific site in preparation for potential disasters [18–21]. Several researchers have performed PSA for various types of disasters [22–24]. Kancev et al. researched the PSA of substation power systems [22]. Salman and Li studied the methodology for seismic PSA of power systems [23]. Furthermore, Wang et al. investigated the PSA of NPP substations for typhoon-induced high winds [24]. Huang and Wang conducted a study to perform real-time risk prediction of regional-scale power systems [25]. However, research on PSA for off-site power systems supplying power to NPPs is limited.

This study performed a PSA of an off-site power system for typhoon-induced high winds, considering the failure correlation between transmission towers. The response correlation based on the distance between transmission towers was analyzed using observational data from automatic weather stations (AWS). The failure correlation between transmission towers due to typhoon-induced high winds was derived using results from the Seismic Safety Margins Research Program (SSMRP) [26]. This correlation was applied to the Kori site, which many failed by typhoons among NPP sites in Korea, to derive quantitative risk results. The fragility of the off-site power system was determined by applying the failure correlation between transmission towers. The probability of the off-site power system failing to supply power to the NPP was calculated by convolving the typhoon hazard of the target site with the fragility of the off-site power system.

2. Derivation of the failure correlation between transmission towers

The off-site power system comprises transmission towers, transmission lines (transmission towers and cables), substations, and power plants other than the target NPP. According to Salman and Li, transmission towers are more vulnerable to wind than earthquakes, whereas substations and power plants are more vulnerable to earthquakes than wind [23]. Therefore, only transmission towers were considered for wind-induced failure to the components of the off-site power system. There have been cases where multiple transmission towers in the power system failed due to the impact of typhoon-induced high winds. Considering that the wind speeds applied to the transmission towers are similar, the probability of failure to the transmission towers due to typhoon-induced high winds may correlate.

The failure correlation between transmission towers due to typhoon-induced high winds was derived using the failure correlation equation from the SSMRP, as shown in Eq. (1) [26].

$$\rho_{12} = \frac{\beta_{R1}\beta_{R2}}{\sqrt{\beta_{R1} + \beta_{C1}\sqrt{\beta_{R2} + \beta_{C2}}}}\rho_{R1R2} + \frac{\beta_{C1}\beta_{C2}}{\sqrt{\beta_{R1} + \beta_{C1}\sqrt{\beta_{R2} + \beta_{C2}}}}\rho_{C1C2} \quad (1)$$

Eq. (1) derives the failure correlation (ρ_{12}) between two transmission towers due to typhoon-induced high winds. To calculate this, the response correlation (ρ_{R1R2}) and wind performance correlation (ρ_{C1C2}) to typhoon-induced high winds between the two transmission towers are required. In addition, the standard deviations of the lognormal distributions of the typhoon-induced high wind response (β_{R1}, β_{R2}) and wind performance (β_{C1}, β_{C2}) for each transmission tower are required.

2.1. Methods of the failure correlation between transmission towers

The response of the transmission towers was obtained by performing a wind analysis using SAP2000. The transmission towers were assumed to be located at the positions of the AWS [27]. The maximum wind speed recorded at the AWS during the duration of the typhoon was used, and the analysis was conducted by dividing the wind direction into intervals of 0° – 90° at 30° increments, as the transmission tower model was

symmetrical [28]. To derive the transmission tower response under the same conditions, the roughness coefficient and amplification factor were set to 1.0. The gust factor used was 1.38, and the roughness classification was set as B [29,30]. The average square root of sum of squares response of the transmission tower was calculated as the Square Root of Sum of Squares (SRSS) response of the displacements in the x-, y-, and z-axes at the four uppermost points of the transmission tower, and the average of these four points was used. The points used to derive the response of the transmission tower are shown in Fig. 1. The response of the transmission tower was determined to be the largest among the average SRSS responses for each wind direction. The correlation was derived from the responses of the two transmission towers and was sorted according to the distance to derive the response correlation between the transmission towers. The method for deriving the response correlation according to the distance between transmission towers is shown in Fig. 2. The transmission tower models were combined into six cases, as detailed below. The correlation was represented as histograms at 50 km intervals for the distance, and the average correlation value was calculated for each interval.

- Case 1: 154 kV vs. 154 kV Transmission tower model
- Case 2: 154 kV vs. 345 kV Transmission tower model
- Case 3: 154 kV vs. 765 kV Transmission tower model
- Case 4: 345 kV vs. 345 kV Transmission tower model
- Case 5: 345 kV vs. 765 kV Transmission tower model
- Case 6: 765 kV vs. 765 kV Transmission tower model

2.1.1. Wind speed data

Wind speed data from the AWS, provided by the Korea Meteorological Administration (KMA), spanning 1991–2022, were used [27]. If the number of AWS data points is small, the correlation is derived as 1. Therefore, only AWS with >30 typhoons in the wind speed data were used. Furthermore, the AWS locations were selected from points that did not change between 1991 and 2022 [27]. Approximately 72 stations were selected, and their locations are shown in Fig. 3. The duration of the typhoons was determined using the Regional Specialized Meteorological Center (RSMC) typhoon data, and the maximum time during which the typhoon passed through the optimal radius of influence (300 km) for typhoons in Korea was used [28,31]. Fig. 4 shows the distribution of the duration of typhoons that occurred within the radius of influence of the Korean Peninsula. The maximum duration of typhoons passing through the Korean Peninsula was 69 h. In the wind speed data,

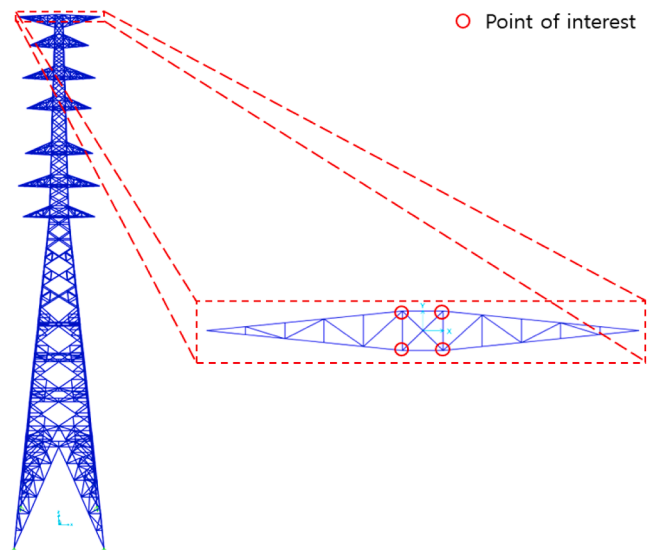


Fig. 1. Points for Deriving Transmission Tower Response.

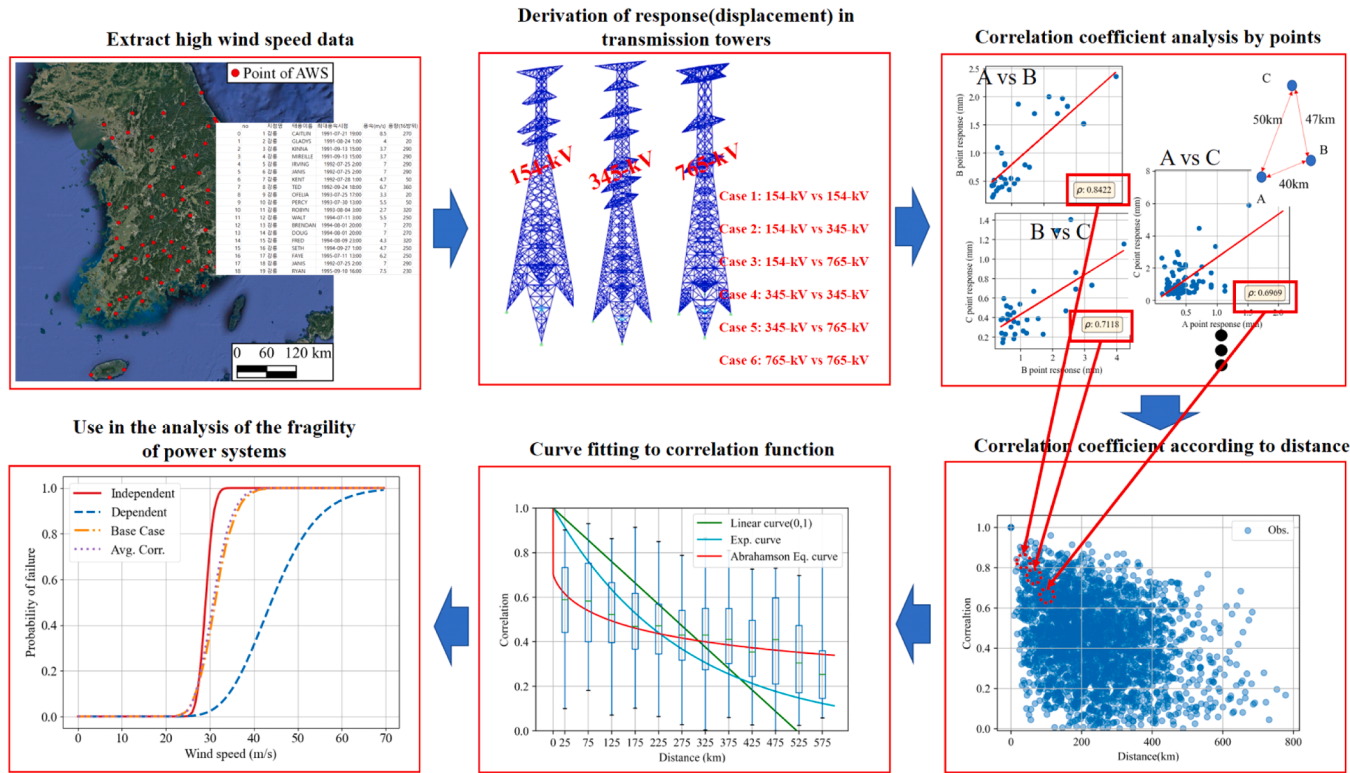


Fig. 2. Method for Deriving Correlation According to Distance.

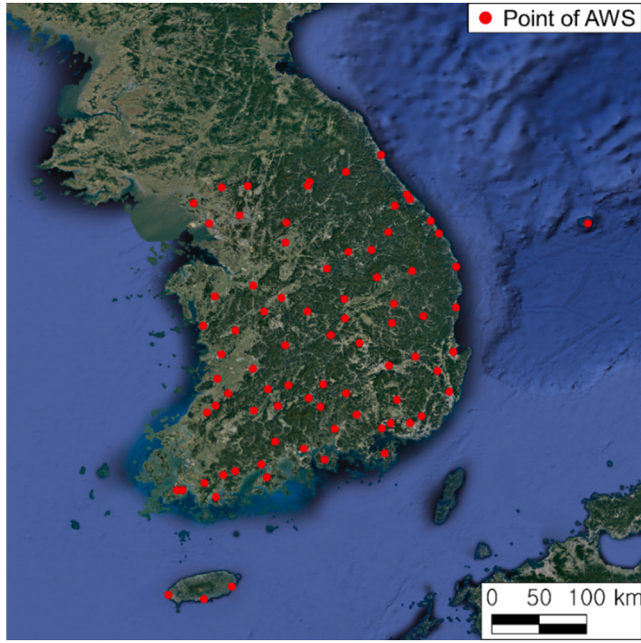


Fig. 3. Locations of Automatic Weather Stations in South Korea.

the time (D) at which the highest wind speed was observed at any AWS during each typhoon was recorded as the time of occurrence. The highest wind speed observed at each AWS during the typhoon's maximum duration was used as the maximum wind speed data. Wind speed data from $D \pm 36$ h were used to obtain more observation data than the maximum duration [27].

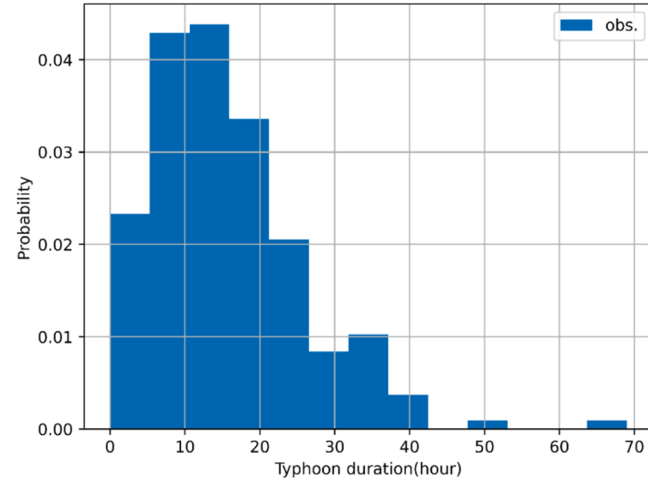


Fig. 4. Duration of Typhoons within the Radius of Influence of the Korean Peninsula.

2.1.2. Transmission tower model

South Korea's commonly constructed transmission tower models are 154, 345, and 765 kV [29]. The 765 kV transmission towers are used to transmit power to large-scale residential complexes and demand areas, whereas the 345 kV transmission towers are used for inter-regional trunk lines and large-scale supply networks in urban areas [28]. There are two types of cross-sections for the structural members of transmission towers: angle-type and pipe-type. This study used angle-type transmission towers of 154, 345, and 765 kV from Park et al.'s transmission tower models [28]. The transmission towers were modeled in SAP2000 using beam-column elements. The material of the transmission towers is A36 steel, with an elastic modulus of 200 GPa, a Poisson's ratio of 0.3, and a density of 7849 kg/m³. The transmission towers used in this

study are shown in Fig. 5, and their characteristics are presented in Table 1 [28].

2.2. Results of the failure correlation between transmission towers

The regression equations for the correlation of the response according to the distance between transmission towers were curve-fitted using three equations. Eqs. (2) and 3 are linear and exponential functions, respectively. Eq. (4) uses the function developed by Abrahamson to derive the correlation between ground motions at different locations [26]. When the distance between transmission towers was 0 km, the exact locations were compared, and the correlation was set to 1.

$$\rho_R = aR + 1 \quad (2)$$

$$\rho_R = a^R + b \quad (3)$$

$$\rho_R = \left(1 + \left(\frac{R \cdot \tanh(d \cdot e)}{a \cdot b} \right)^f \right)^{-1/2} \cdot \left(1 + \left(\frac{R \cdot \tanh(d \cdot e)}{a \cdot c} \right)^g \right)^{-1/2} \quad (4)$$

where, R: distance between transmission towers

a ~ g: parameters to be fitted

The results were evaluated after curve fitting the response correlation according to the distance between transmission towers using three regression equations. Table 2 shows the average of the response correlation coefficient for each distance interval between the transmission towers. Table 3 shows the variance of the response correlation coefficient for each distance interval between the transmission towers. The results fitted to the regression curves, root mean square error (RMSE) values, and the corresponding regression model parameters are presented in Tables 4–9. Furthermore, the response correlation according to the distance between transmission towers and the corresponding regression curves are shown in Figs. 6–11. In all analyzed cases, the response correlation by distance exhibited characteristics of a normal distribution between 0 and 300 km. Among the various regression models, Abrahamson's equation showed the best performance in terms of RMSE. For the regression equations of the linear and exponential functions fitted to the mean correlation by interval, the R^2 values were below 0.5, whereas the curve derived using Abrahamson's equation had the highest R^2 value of 0.98.

The regression curve using Abrahamson's equation had the lowest

Table 1

Characteristics of Transmission Tower Models [28].

Category	Dimension		Cable load		
	Height (m)	Width (m)	Unit weight (kgf/m)	Span length (m)	Number of cables
154 kV	62.0	14.5	1.836	500	4
345 kV	122.8	19.8	1.637	450	4
765 kV	155.5	26.7	1.637	400	4

Table 2

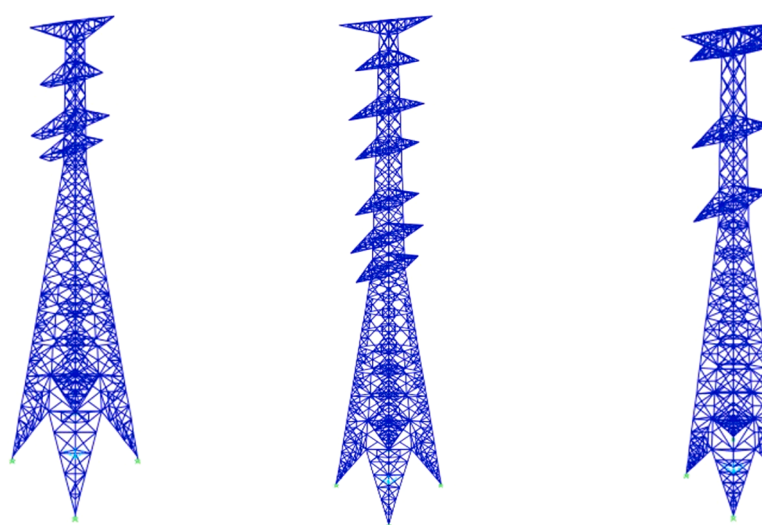
Average of Correlation Coefficient by Response Interval According to Distance Between Transmission Towers.

Bin(km)	Average of Correlation Coefficient					
	Case 1	Case 2	Case 3	Case 4	Case 5	Case 6
0	1.00	0.99	0.99	1.00	0.99	1.00
0–50	0.57	0.57	0.57	0.57	0.57	0.57
50–100	0.52	0.52	0.52	0.52	0.52	0.52
100–150	0.48	0.48	0.48	0.48	0.48	0.48
150–200	0.43	0.43	0.43	0.43	0.43	0.43
200–250	0.41	0.41	0.41	0.41	0.41	0.41
250–300	0.41	0.41	0.41	0.41	0.41	0.41
300–350	0.39	0.39	0.39	0.39	0.39	0.39
350–400	0.38	0.38	0.38	0.38	0.38	0.38
400–450	0.31	0.31	0.31	0.31	0.31	0.31

Table 3

Variance of Correlation Coefficient by Response Interval According to Distance Between Transmission Towers.

Bin(km)	Variance of Correlation Coefficient					
	Case 1	Case 2	Case 3	Case 4	Case 5	Case 6
0	0.00	0.00	0.00	0.00	0.00	0.00
0–50	0.18	0.18	0.17	0.18	0.18	0.18
50–100	0.18	0.19	0.18	0.18	0.19	0.19
100–150	0.18	0.18	0.18	0.18	0.18	0.18
150–200	0.20	0.20	0.20	0.20	0.21	0.20
200–250	0.18	0.18	0.18	0.18	0.18	0.18
250–300	0.19	0.19	0.19	0.19	0.19	0.19
300–350	0.17	0.17	0.17	0.17	0.17	0.17
350–400	0.18	0.17	0.17	0.18	0.18	0.17
400–450	0.17	0.17	0.17	0.17	0.17	0.17



(a) 154 kV transmission tower (b) 345 kV transmission tower (c) 765 kV transmission tower

Fig. 5. Transmission Towers Models [28].

Table 4

Fitted parameters and RMSE results with correlation for Case 1.

Parameters	Linear Equation	Exponential Equation	Abrahamson's Equation
A	-2.33E-03	9.96E-01	6.78E+00
B	-	1.00E+0	5.10E-02
C	-	-	3.42E+00
D	-	-	2.05E-01
E	-	-	2.05E-01
F	-	-	4.63E-01
G	-	-	6.37E+00
RMSE	0.286	0.232	0.191
R ²	0.123	0.248	0.982

Table 5

Fitted parameters and RMSE results with correlation for Case 2.

Parameters	Linear Equation	Exponential Equation	Abrahamson's Equation
A	-2.33E-03	9.96E-01	6.13E+00
B	-	1.00E+0	4.98E-01
C	-	-	4.88E+00
D	-	-	5.74E-01
E	-	-	5.74E-01
F	-	-	2.63E-16
G	-	-	7.41E-01
RMSE	0.288	0.234	0.193
R ²	0.119	0.243	0.975

Table 6

Fitted parameters and RMSE results with correlation for Case 3.

Parameters	Linear Equation	Exponential Equation	Abrahamson's Equation
a	-2.33E-03	9.96E-01	3.89E+00
b	-	-	2.46E+00
c	-	-	1.04E+01
d	-	-	6.77E-01
e	-	-	6.77E-01
f	-	-	4.91E-12
g	-	-	7.40E-01
RMSE	0.288	0.234	0.193
R ²	0.119	0.243	0.975

Table 7

Fitted parameters and RMSE results with correlation for Case 4.

Parameters	Linear Equation	Exponential Equation	Abrahamson's Equation
a	-2.33E-03	9.96E-01	7.08E+00
b	-	1.00E+0	7.10E-01
c	-	-	8.09E+00
d	-	-	8.40E-01
e	-	-	8.40E-01
f	-	-	1.86E-06
g	-	-	7.41E-01
RMSE	0.286	0.232	0.191
R ²	0.123	0.244	0.978

Table 8

Fitted parameters and RMSE results with correlation for Case 5.

Parameters	Linear Equation	Exponential Equation	Abrahamson's Equation
a	-2.33E-03	9.96E-01	9.68E+00
b	-	1.00E+0	6.80E-02
c	-	-	4.57E+00
d	-	-	2.83E-01
e	-	-	2.83E-01
f	-	-	4.63E-01
g	-	-	6.36E+00
RMSE	0.288	0.234	0.193
R ²	0.123	0.247	0.984

Table 9

Fitted parameters and RMSE results with correlation for Case 6.

Parameters	Linear Equation	Exponential Equation	Abrahamson's Equation
a	-2.33E-03	9.96E-01	4.35E+00
b	-	1.00E+0	7.19E-01
c	-	-	9.92E+00
d	-	-	7.03E-01
e	-	-	7.03E-01
f	-	-	6.47E-11
g	-	-	7.39E-01
RMSE	0.286	0.232	0.191
R ²	0.123	0.248	0.977

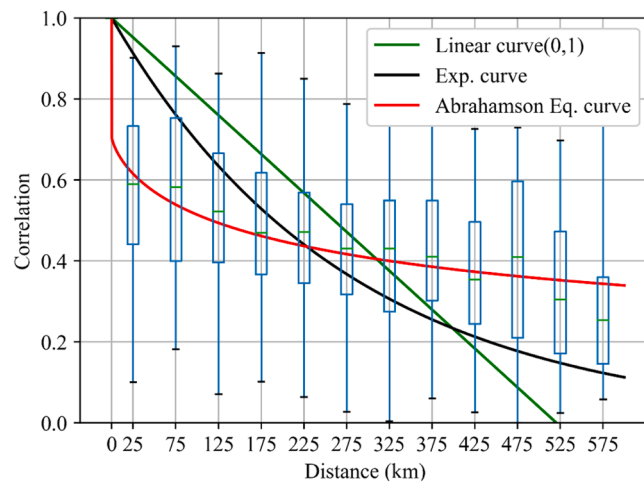


Fig. 6. Correlation according to distance for transmission tower response in Case 1.

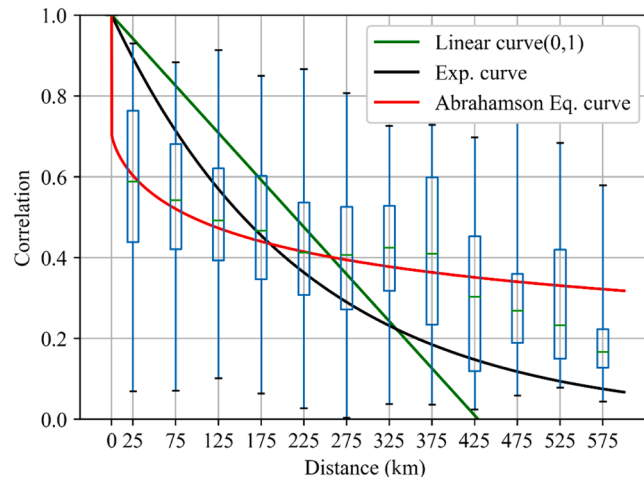


Fig. 7. Correlation according to distance for transmission tower response in Case 2.

RMSE values among the three regression curves for the response correlation according to the distance between the transmission towers, with RMSE values of 0.191, 0.193, 0.193, 0.191, 0.193, and 0.191, respectively. Abrahamson's equation was the closest to the mean curve compared to the linear and exponential equations. Moreover, Abrahamson's equation exhibited the best performance in terms of R². Therefore, Abrahamson's equation was selected as the correlation for the base case. The failure correlation from typhoon-induced high winds was derived through the SSMRP equation using the response correlation according to the distance between transmission towers. A PSA of the

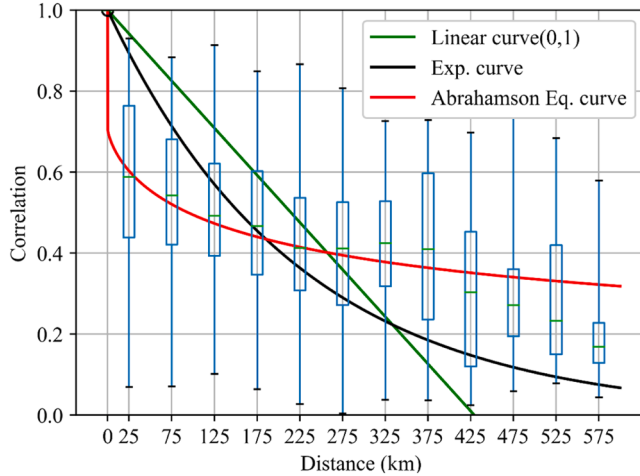


Fig. 8. Correlation according to distance for transmission tower response in Case 3.

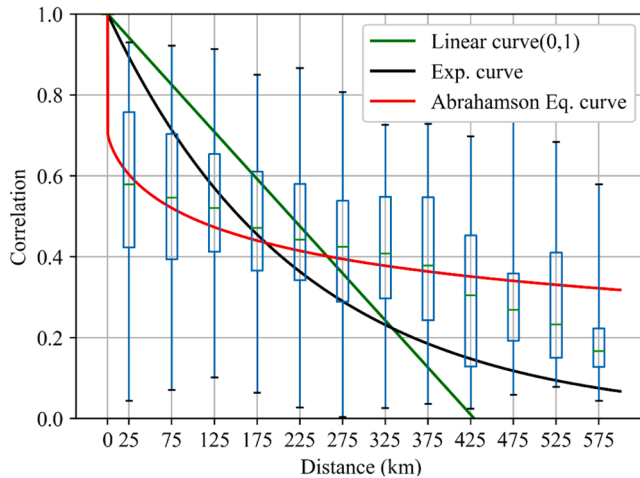


Fig. 9. Correlation according to distance for transmission tower response in Case 4.

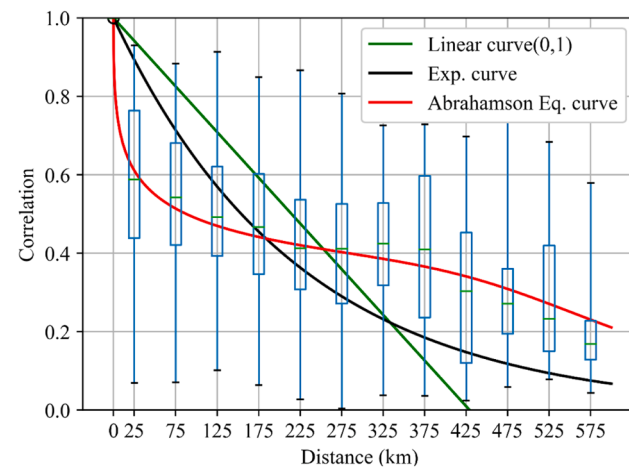


Fig. 10. Correlation according to distance for transmission tower response in Case 5.

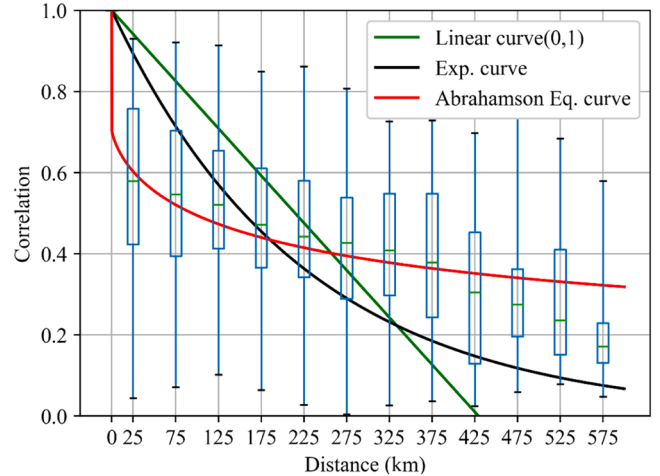


Fig. 11. Correlation according to distance for transmission tower response in Case 6.

power system considering the failure correlation was performed, and the changes owing to the consideration of a realistic correlation were derived through quantitative risk results.

[Table 5](#), [Table 6](#), [Table 7](#), [Table 8](#), [Table 9](#)

3. Probabilistic safety assessment of the off-site power system due to typhoon-induced high winds considering failure correlation

The PSA of the off-site power system due to typhoon-induced high winds follows this procedure [32]. First, the typhoon hazard for the target site in the specified area is determined. Next, the fragility of the off-site power system is analyzed based on the fragility of its components to high winds. Finally, the risk is calculated by convolving the typhoon hazard with the power system's fragility. Fig. 12 illustrates the conceptual PSA process for the power system due to typhoon-induced high winds.

$$\text{Risk} = \int_{-\infty}^{\infty} P_f(a) \left| \frac{dH(a)}{da} \right| da \quad (5)$$

where, a : Wind speed

$P_f(a)$: Fragility of off-site power system
 $H(a)$: Typhoon hazard curve

A PSA of the off-site power system due to typhoon-induced high winds was conducted for the Kori site, which experienced the most severe failure of the off-site power system due to typhoons or high winds among domestic NPPs from 1978 to 2021 [10]. The typhoon hazard for the Kori site was obtained from the results of Kim et al. [33]. The off-site power system near the Kori NPP site was constructed, and the fragility was set and analyzed based on the power system components.

Fragility was set for the components constituting the power system, and the fragility of the off-site power system was analyzed. The fragility analysis of the off-site power system was performed by considering the correlation between the power system components, using the failure correlation of independent, totally dependent, partially dependent. There are four cases, as stated below. Based on the PSA method of the off-site power system due to typhoon-induced high winds, the annual probability of the off-site power system failing to provide power to the Kori NPP site was analyzed.

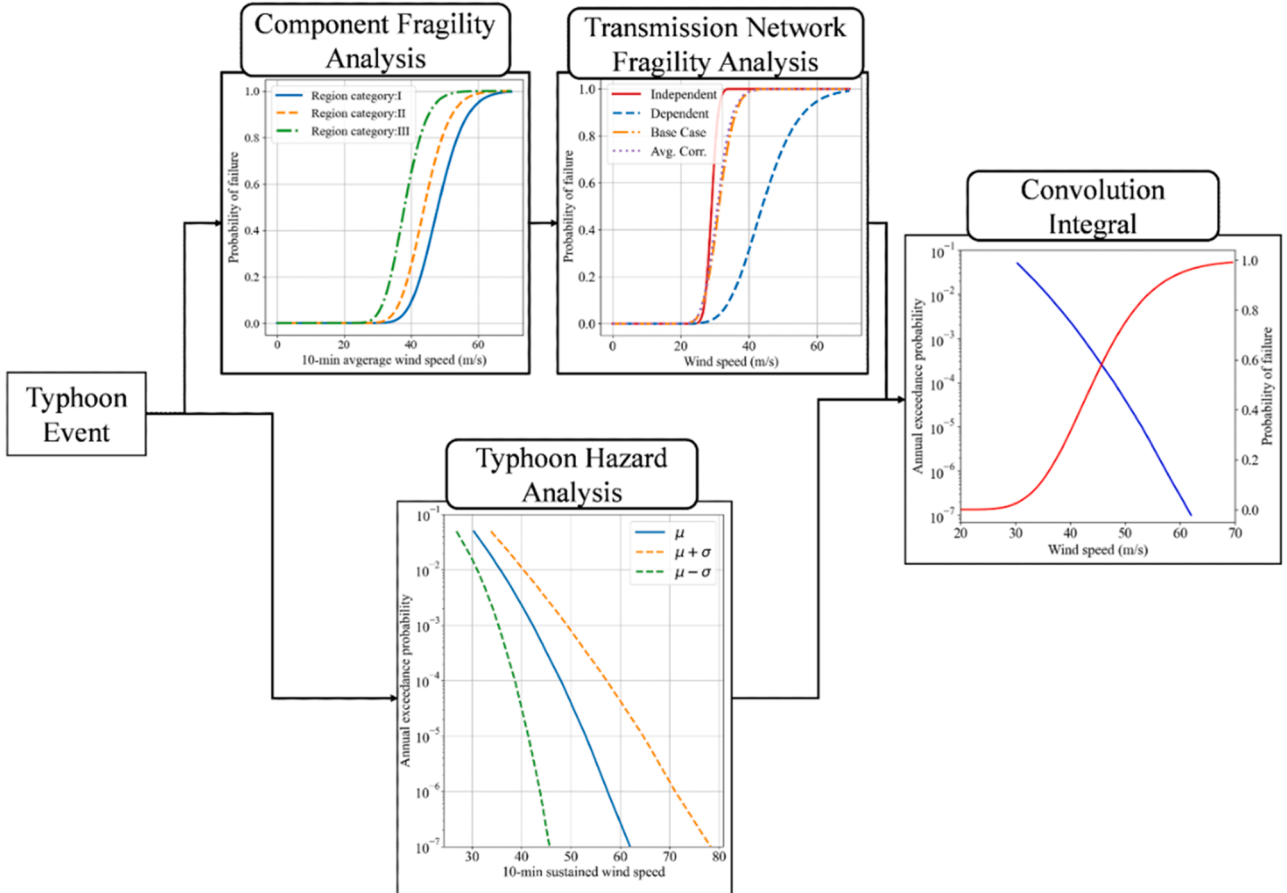


Fig. 12. Typhoon PSA process.

Case 1: The failure correlation coefficient between transmission towers is independent

Case 2: The failure correlation coefficient between transmission towers is totally dependent

Case 3 (Base case, partially dependent): Failure correlation between transmission towers using Abrahamson's equation

Case 4 (Avg. Corr., partially dependent): Average failure correlation in the 0–50 km range

3.1. Construction of the off-site power system

The off-site power system for the Kori NPP site was constructed with a radius of 30 km centered on the Kori NPP site, and the layout of the constructed off-site power system is shown in Fig. 13. The total number of nodes in the constructed power system was 1520, with nodes outside the 30 km radius assumed to remain operational. Furthermore, substations and power plants were assumed to be unaffected by typhoon-induced high winds.

3.2. Typhoon hazard of the kori npp and wind fragility of transmission towers

To conduct a PSA of the off-site power system due to typhoon-induced high winds, both the risk of typhoon-induced high winds and the fragility of the off-site power system must be assessed. The typhoon-induced high wind hazard for the Kori NPP site was obtained from the study by Kim et al., as shown in Fig. 14 [11].

The fragility of each power system component is required to derive the fragility of the off-site power system. The components of the off-site

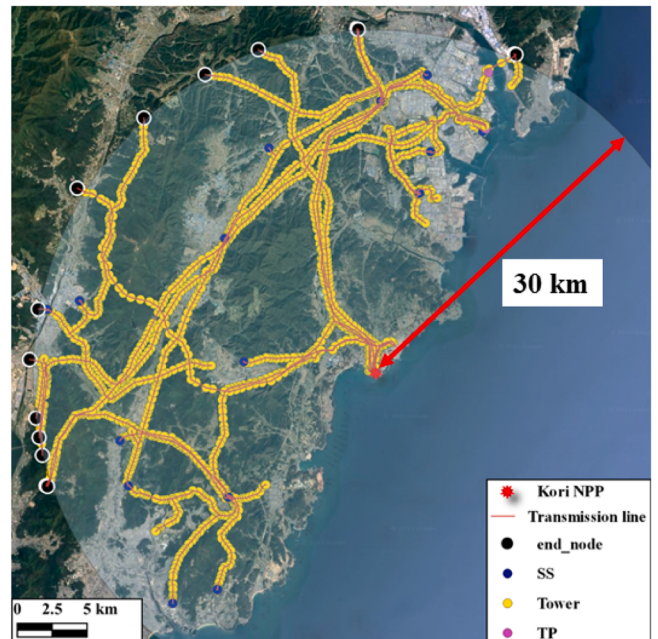


Fig. 13. Constructed off-site power system.

power system include power plants, substations, and transmission lines. In this safety assessment, only transmission lines were considered for assessment, as power plants and substations are not vulnerable to wind loads [23]. The fragility of transmission lines was selected based on the

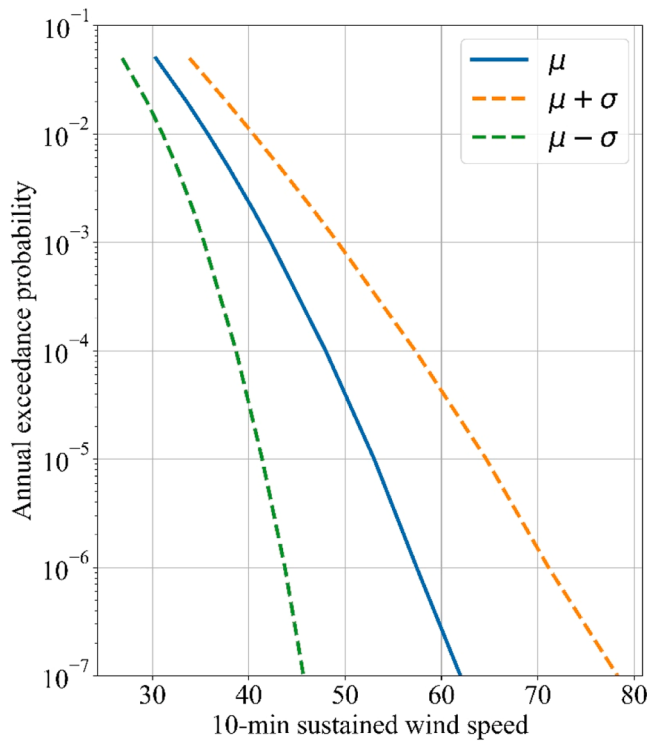


Fig. 14. Typhoon-induced high wind hazard for the kori NPP site [11].

high wind fragility of SSCs in NPPs from Ravindra's study, as shown in Eq. (6) [34]. The design wind speed " V_d " is necessary to derive the fragility of transmission lines. The design criteria for overhead transmission towers in South Korea (DS-1111) provide the design standards for the reference velocity pressure and maximum wind speed based on regional classifications [29]. Table 10 displays the design wind speeds provided in DS-1111, and Fig. 15 shows the regional classifications.

$$V_m = \sqrt{1.1 \cdot 1.2 \cdot V_d^2}, \beta_r = 0.1, \beta_u = 0.15 \quad (6)$$

where, V_m : median wind speed

V_d : design wind speed

β_r : logarithmic standard deviations for randomness

β_u : logarithmic standard deviations for uncertainty

The performance correlation coefficient is generally independent [35]. Therefore, in this study, we assumed the performance correlation coefficient between transmission towers to be '0'. And, in this study, the logarithmic standard deviation value proposed by Ravindra was used to derive the wind fragility of transmission lines. However, Ravindra did not provide separate logarithmic standard deviations for response and performance. Therefore, this study assumed that the logarithmic standard deviation of wind performance and response is the same, which could result in errors in the network risk due to the failure correlation

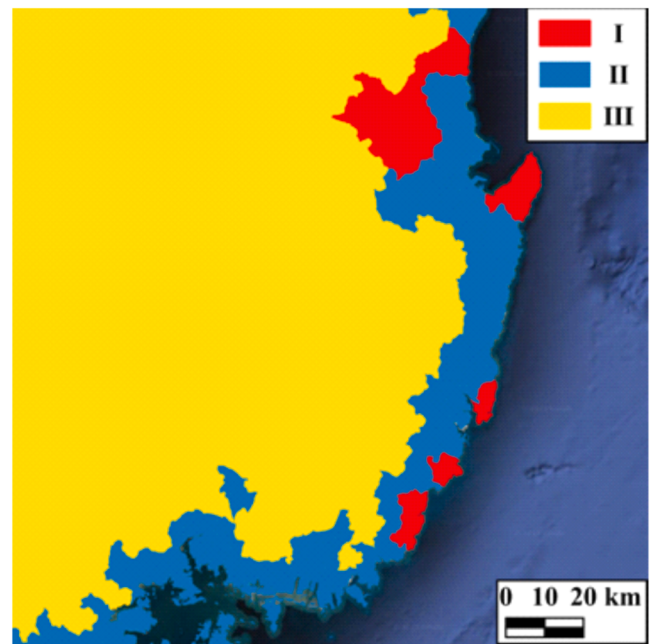


Fig. 15. Regional classification presented in DS-1111[29].

coefficient between transmission towers.

3.3. Probabilistic safety assessment results and discussion

The fragility of the power system was derived using a risk analysis program developed by Eem, the operation method of which is shown in Fig. 16 [36,37]. Sampling was conducted over 8000 times to assess the fragility of the off-site power system. The fragility curves using the correlation for the four cases are shown in Fig. 17, and the high confidence of low probability of failure (HCLPF) and " V_m " are presented in Table 11. The constructed power system was a complex network of OR and AND conditions. The HCLPF was lowest in Case 3, and the wind speed at 50 % probability of failure, or the median wind speed, was 31.14 m/s, which was higher than the results using only totally dependent and average correlation. The derived fragility results for the off-site power system were convolved with the typhoon hazard of the Kori NPP site.

A PSA of the off-site power system due to typhoon-induced high winds was conducted, considering the failure correlation. This assessment quantitatively determined the probability of the Kori NPP site being unable to receive power supply due to typhoon-induced high winds. The HCLPF for each case was calculated, and the error rate was determined based on Case 3.

When the correlation coefficient of the failure probability between transmission towers is used independent (Case 1), HCLPF is 25.53 m/s, and the risk is 4.79E-2/yr. Using totally dependent (Case 2), the HCLPF is 28.09 m/s, and the risk is 5.03E-3/yr. Using the Abrahamson equation (Case 3), the HCLPF is 23.47 m/s, and the risk is 3.40E-2/yr. Using the average correlation coefficient between transmission towers (Case 4), the HCLPF is 23.68 m/s, and the risk is 3.59E-2/yr.

The error ratios of HCLPF and risk are shown in Table 12 based on Case 3. In Case 1, HCLPF is about 8.8 % higher, and the risk is 40.98 % higher than in Case 3. In Case 2, HCLPF is about 19.69 % higher, and the risk is 85.20 % higher than Case 3. In Case 4, HCLPF is about 0.88 % higher, and the risk is 5.46 % higher than Case 3.

The failure probability showed a tendency to decrease when considering the failure correlation coefficient compared to assuming the failure probability between transmission towers to be independent. This is likely because most transmission lines are composed of Or gates. According to the study by Eem et al., as the failure correlation coefficient

Table 10

Design wind speeds for overhead transmission towers by regional classification [29,34].

Region category	Velocity pressure (kg/m^2)	Maximum wind speed (m/s)		Gust factor
		10-min average	3- sec Gust	
I	117	40.0	54.0	1.35
II	100	36.6	50.0	1.37
III	76	31.7	43.7	1.38

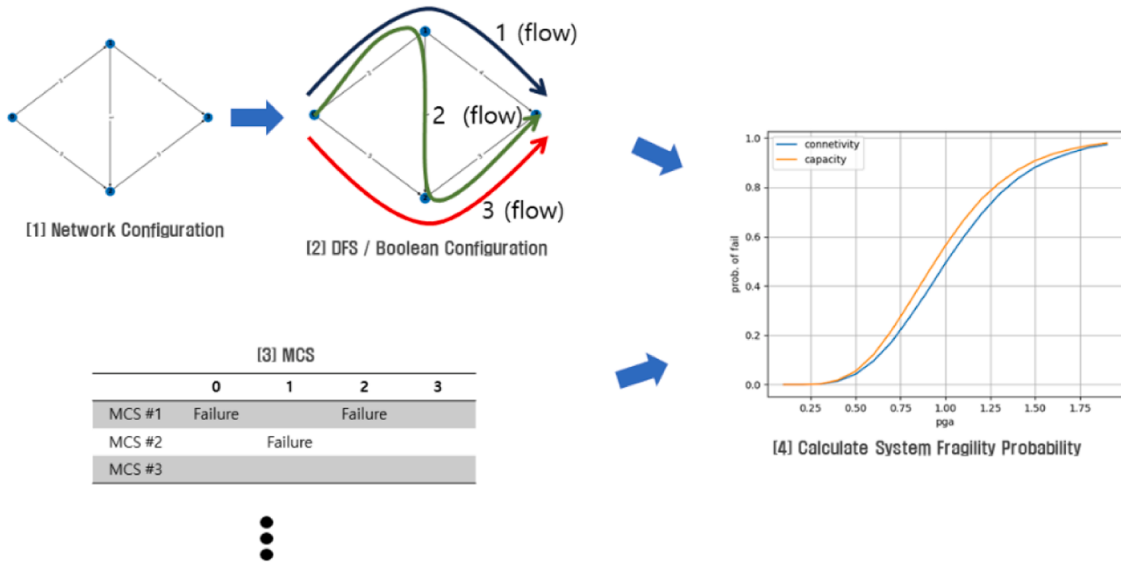


Fig. 16. Method of the risk analysis program [36,37].

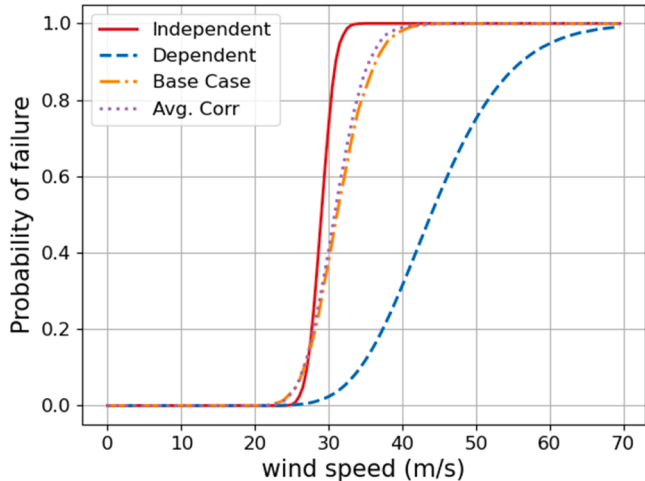


Fig. 17. Fragility curves of the off-site power system.

Table 11
HCLPF and V_m for each case.

Category	HCLPF	V_m
Case 1	25.53	29.02
Case 2	28.09	43.92
Case 3	23.47	31.14
Case 4	23.68	30.81

Table 12
HCLPF and risk for each case.

Category	HCLPF	HCLPF error ratio (%)	Risk (/yr)	Risk error ratio (%)
Case 1	25.53	8.80	4.79×10^{-2}	40.98
Case 2	28.09	19.69	5.03×10^{-3}	85.20
Case 3	23.47	0.00	3.40×10^{-2}	0.00
Case 4	23.68	0.88	3.59×10^{-2}	5.46

increases, the failure probability increases in an And gate and decreases in an Or gate [38]. Failure probability of the constructed power system is expected to be more dominated by Or gates than And gates.

Assuming that the failure probabilities between transmission towers

are independent or totally dependent, there is a significant difference compared to the results obtained by applying the failure correlation coefficient. In reality, the probability of failure of power systems due to typhoons is correlated. Therefore, an assessment considering the correlation coefficient of failure probability (as in Case 3) is more realistic. Additionally, the evaluation using the average correlation coefficient of the damage probabilities between transmission towers (Case 4) produced results similar to those of Case 3, suggesting that using the average correlation coefficient is also effective.

4. Conclusion

Recently, the intensity and frequency of typhoons have increased, and typhoons can cause LOOP events in NPPs. LOOP events can affect the safety of NPPs. To safely operate an alienated power system, evaluating its safety against typhoon-induced high winds is essential. PSA requires both typhoon hazards and the fragility of the off-site power system components. There have been cases where multiple transmission towers simultaneously failed because of typhoon-induced high winds. When performing a PSA of an off-site power system, considering the correlation between the components constituting the off-site power system can result in a realistic safety assessment. This study performed a PSA of an off-site power system, considering the failure correlation between transmission towers. Ultimately, the probability of the off-site power system failing to supply electricity to the NPP was derived.

The response correlation according to the distance between transmission towers was analyzed. Regression curves were produced by curve fitting the derived response correlation according to distance to the three regression equations. The distance was divided into intervals, and the average distribution of the response correlation was derived. Among the correlations according to distance, the regression curve fitted to Abrahamson's equation showed the best RMSE and R^2 values compared to the other two regression curves. Using the regression curve fitted to Abrahamson's equation will enable a more realistic assessment compared to the other two regression equations.

The PSA of the off-site power system at the Kori NPP site was performed by applying the failure correlation of typhoon-induced high winds. This correlation can be calculated using the SSMRP equation, which considers the response and wind performance correlation according to the distance between transmission towers, assuming the wind performance correlation to be zero. The fragility of the power system was then derived by applying the failure correlation of typhoon-induced high winds. In the PSA results, the risk was lowest when totally

dependent was assumed and highest when independence was assumed. The safety assessment result, applying the failure correlation of typhoon-induced high winds between transmission towers using Abrahamson's equation, was derived as 3.40E-2/yr. This result showed significant differences of 40.98 % and 85.20 % compared with the safety assessment results assuming independent and totally dependent, respectively. Applying the failure correlation of typhoon-induced high winds in the PSA of an off-site power system is deemed more realistic. When applying the failure correlation of typhoon-induced high winds through the average response correlation between transmission towers by interval, the safety assessment result was 3.59E-2, with an error of approximately 5 %. However, it can be used for efficient calculations.

CRediT authorship contribution statement

Gungyu Kim: Writing – original draft, Formal analysis. **Shinyoung Kwag:** Writing – review & editing, Validation, Investigation. **Seunghyun Eem:** Writing – review & editing, Writing – original draft, Visualization, Validation, Supervision, Software, Resources, Project administration, Methodology, Investigation, Funding acquisition, Formal analysis, Data curation, Conceptualization. **Dae-gi Hahn:** Writing – review & editing, Supervision, Project administration, Investigation, Data curation. **Jin Hee Park:** Writing – review & editing, Methodology, Investigation, Conceptualization.

Declaration of competing interest

The authors declare that they have no known competing financial interests or personal relationships that could have appeared to influence the work reported in this paper.

Acknowledgments

This work was supported by the National Research Foundation of Korea (NRF) grant funded by the Korean Government (Ministry of Science and ICT) (No. RS-2022-00154571).

Data availability

Data will be made available on request.

References

- [1] World Meteorological Organization (WMO). Atlas of mortality and economic losses from weather, climate and water extremes (1970–2012). 2021.
- [2] World Meteorological Organization (WMO). Notable tropical cyclones <https://public.wmo.int/en/our-mandate/focus-areas/natural-hazards-and-disaster-risk-reduction/tropical-cyclones/Notable-tcs> [accessed April 4, 2024].
- [3] World Meteorological Organization (WMO). Tropical Cyclones n.d. <https://public.wmo.int/en/our-mandate/focus-areas/natural-hazards-and-disaster-risk-reduction/tropical-cyclones> [accessed April 4, 2024].
- [4] Bae Y.J., Lee H.J., Jung B.W. Korean Climate Change Assessment Report 2020 -Climate Impact and Adaptation-. Sejong-Si: 2020.
- [5] Choun YS, Kim MK. Logic tree approach for probabilistic typhoon wind hazard assessment. Nuc Engineer Technol 2019;51:607–17. <https://doi.org/10.1016/J.NET.2018.11.006>.
- [6] Dikshit S, Alipour A. A moment-matching method for fragility analysis of transmission towers under straight line winds. Reliab Eng Syst Saf 2023;236: 109241. <https://doi.org/10.1016/j.ress.2023.109241>.
- [7] Yoon JY, Kim DS, Han SH. A practical approach to treating time dependencies between diesel generator failures and offsite power recovery in multi-unit PSA. Reliab Eng Syst Saf 2024;245:110013. <https://doi.org/10.1016/J.RESS.2024.110013>.
- [8] Kopytko N, Perkins J. Climate change, nuclear power, and the adaptation–mitigation dilemma. Energy Policy 2011;39:318–33.
- [9] Electric Power Research Institute (EPRI). High-Wind Risk Assessment Guidelines, TR-3002003107. 2015.
- [10] Korea Institute of Nuclear Safety (KINS). Safety information by sector. Korea Institute of Nuclear Safety (KINS) n.d. <https://nsic.nssc.go.kr/information/reguDataActive.do?nsicDtaTyCode=nppAccident> (Accessed April 4, 2024).
- [11] Huang X, Wang N. An adaptive nested dynamic downscaling strategy of wind-field for real-time risk forecast of power transmission systems during tropical cyclones. Reliab Eng Syst Saf 2024;242:109731. <https://doi.org/10.1016/j.ress.2023.109731>.
- [12] Macedo FC, Alminhana F, Fadel Miguel LF, Beck AT. Performance-based reliability assessment of transmission lines under tornado actions. Reliab Eng Syst Saf 2024; 252:110475. <https://doi.org/10.1016/j.ress.2024.110475>.
- [13] Zhang J, Xie Q. Failure analysis of transmission tower subjected to strong wind load. J Constr Steel Res 2019;160:271–9. <https://doi.org/10.1016/J.JCSR.2019.05.041>.
- [14] An L, Wu J, Zhang Z, Zhang R. Failure analysis of a lattice transmission tower collapse due to the super typhoon Rammasun in July 2014 in Hainan Province, China. J Wind Engineer Indust Aerodynamic 2018;182:295–307. <https://doi.org/10.1016/J.JWEIA.2018.10.005>.
- [15] Bi W, Tian L, Li C, Ma Z, Pan H. Wind-induced failure analysis of a transmission tower-line system with long-term measured data and orientation effect. Reliab Eng Syst Saf 2023;229:108875. <https://doi.org/10.1016/j.ress.2022.108875>.
- [16] Eem S-H, Choi I-K. Influence analysis of seismic risk due to the failure correlation in seismic probabilistic safety assessment. J Earthquake Engineer Soc Korea 2019; 23:101–8. <https://doi.org/10.5000/EESK.2019.23.2.101>.
- [17] Eem S, Kwag S, Choi I-K, Hahn D. Sensitivity analysis of failure correlation between structures, systems, and components on system risk. Nucl Engineer Technol 2023;55:981–8. <https://doi.org/10.1016/j.net.2022.10.043>.
- [18] Al-Douri A, Levine CS, Groth KM. Identifying human failure events (HFEs) for external hazard probabilistic risk assessment. Reliab Eng Syst Saf 2023;235: 109236. <https://doi.org/10.1016/j.ress.2023.109236>.
- [19] Zhou T, Zhang L, Hu J, Modarres M, Drogueut EL. A critical review and benchmark study of dependency modeling for seismic probabilistic risk assessment in the nuclear power industry. Reliab Eng Syst Saf 2024;245:110009. <https://doi.org/10.1016/j.ress.2024.110009>.
- [20] Cho J, Lee SH, Kim J, Park SK. Framework to model severe accident management guidelines into Level 2 probabilistic safety assessment of a nuclear power plant. Reliab Eng Syst Saf 2022;217:108076. <https://doi.org/10.1016/j.ress.2021.108076>.
- [21] Yoon JY, Kim D-S, Han SH. A practical approach to treating time dependencies between diesel generator failures and offsite power recovery in multi-unit PSA. Reliab Eng Syst Saf 2024;245:110013. <https://doi.org/10.1016/j.ress.2024.110013>.
- [22] Kancev D, Causevski A, Cepin M, Volkanovski A. Application of probabilistic safety assessment for macedonian electric power system. Ljubljana (Slovenia): Nuclear Society of Slovenia; 2007.
- [23] Salman AM, Li Y. A probabilistic framework for seismic risk assessment of electric power systems. Procedia Eng 2017;199:1187–92. <https://doi.org/10.1016/j.proeng.2017.09.324>.
- [24] Wang H, Liang X, Zhang X, Feng B. Study on high wind hazard probability risk assessment methods of nuclear power plant. In: IOP Conf Ser: Earth Environ Sci. 467; 2020, 012075. <https://doi.org/10.1088/1755-1315/467/1/012075>.
- [25] Huang X, Wang N. An adaptive nested dynamic downscaling strategy of wind-field for real-time risk forecast of power transmission systems during tropical cyclones. Reliab Eng Syst Saf 2024;242:109731. <https://doi.org/10.1016/j.ress.2023.109731>.
- [26] Smith PD, Dong RG, Bernreuter DL, Bohn MP, Chuang TY, Cummings GE, et al. Seismic safety margins research program. Phase I Final Rep - Overview 1981.
- [27] Korea Meteorological Administration (KMA). Automatic weather station (AWS) data. Seoul (Republic of Korea): Korea Meteorological Administration; 2023. <https://data.kma.go.kr/data/grnd/selectAwsRltmList.do> [accessed November 20, 2023].
- [28] Park H-S, Choi BH, Kim JJ, Lee T-H. Seismic performance evaluation of high voltage transmission towers in South Korea. KSCE Journal of Civil Engineering 2016;20:2499–505. <https://doi.org/10.1007/s12205-015-0723-3>.
- [29] Korea Electric Power Corporation. Design standard of tower for overhead transmission line, DS-1111 (in Korean). 2013. Korea.
- [30] Korea Construction Standards Center (KCSC). Building design load, kds 41 12 00: 2022. Goyang (Republic of Korea): Korea Construction Standards Center; 2022.
- [31] Cho KH, Kim SC. A study on optimal radius of typhoon selection for Monte Carlo method. In: Proceedings of the Wind Engineering Institute of Korea. Seoul National University; 2009, p. 39–43.
- [32] Kim G, Kwag S, Eem S, Jin S-S. Probabilistic safety assessment of offsite power system under typhoon-induced high wind. KSCE J Civil Environ Engineer Res 2024;44:277–82. <https://doi.org/10.12652/Ksce.2024.44.3.0277>.
- [33] Kim G, Kwag S, Eem S. Correlation Analysis of Wind Speeds for the Wind Safety Assessment in Off-site Power System. In: Transactions of the Korean Nuclear Society Autumn Meeting; 2023.
- [34] Ravindra MK. State-Of-The-Art and Current Research Activities in Extreme Winds Relating to Design And Evaluation of Nuclear Power Plants. In The Tornado. Its Structure, Dynamics, Prediction, and Hazards 1993:389–97. <https://doi.org/10.1029/GM079p0389>.
- [35] Electric Power Research Institute (EPRI). Framework for assessing multi-unit risk to support risk-informed decision-making: general framework and application-specific refinements, TR-3002020765. 2021.
- [36] Eem S. Risk Analysis Program. Version 1.0 [software]. C-2022-015828. 2022. (in Korean).
- [37] Eem S, Kwag S, Hahn D. Development of network evaluation techniques for probabilistic safety assessment of power grid. Yeosu (Republic of Korea): KSCE 2023 Conference & Civil Expo; 2023.
- [38] Eem S, Kwag S, Choi I-K, Hahn D. Sensitivity analysis of failure correlation between structures, systems, and components on system risk. Nucl Engineer Technol 2023;55:981–8. <https://doi.org/10.1016/j.net.2022.10.043>.